

Journal of Theoretical and Computational Chemistry
© World Scientific Publishing Company

Random Phase Approximation For Allowed and Parity Non-conserving Electric Dipole Transition Amplitudes and its Connection with Many-Body Perturbation Theory and Coupled-Cluster Theory

GEETHA GOPAKUMAR

Department of Applied Chemistry, University of Tokyo, Japan.
geetha@qcl.t.u-tokyo.ac.jp
http://www.u-tokyo.ac.jp

CHIRANJIB SUR, BHANU PRATAP DAS, RAJAT K. CHAUDHURI

Indian Institute of Astrophysics, Bangalore, India
csur@iiap.res.in, das@iiap.res.in, rajat@iiap.res.in

DEBASHIS MUKHERJEE

Indian Association for the Cultivation of Science, Kolkata, India
pdm@iacs.res.in

KIMIHIKO HIRAO

Department of Applied Chemistry, University of Tokyo, Japan
hirao@qcl.t.u-tokyo.ac.jp

Received Day Month Year

Revised Day Month Year

Accepted Day Month Year

The connections between the Random Phase Approximation (RPA) and Many-Body Perturbation Theory (MBPT) and its all order generalisation, the Coupled-Cluster Theory (CCT) have been explored. Explicit expressions have been derived for the electric dipole amplitudes for allowed and forbidden transitions induced by the parity non-conserving neutral weak interaction. The Goldstone diagrams associated with the RPA terms in both cases are shown to arise in MBPT and CCT and the numerical verification of this relationship is made for the allowed electric dipole transitions.

Keywords: RPA; MBPT; CC

1. INTRODUCTION

The Random Phase Approximation (RPA) has been successfully used in calculating core polarisation/relaxation effects in a variety of properties¹. It is an approximate many-body theory that has been formulated in a number of different but equivalent ways². However, its connection with MBPT and CCT has not been explored in detail to the best of our knowledge. We focus on this particular point in this paper.

2 *Geetha Gopakumar et al*

The outline of the paper is as follows. We first derive an effective operator in MBPT for electric dipole ($E1$) transition amplitudes for allowed and forbidden transitions induced by the Parity Non Conserving (PNC) neutral current weak interaction³. From the general expression in MBPT, we consider diagrammatically all the RPA diagrams pertaining to zeroth and first order in the residual Coulomb interaction. This is followed by theoretical understanding of these effects starting from Hartree Fock (HF) equations to show how these effects can be represented as linear equations which in turn can be solved to self-consistency taking the residual Coulomb interaction to all orders. At the end, starting from the basic formalism for CC method, we compare the RPA diagrams both theoretically and numerically with the corresponding diagrams in CCT.

2. General form of an effective operator in MBPT

In perturbation theory, the functional space for the wave function is separated into two parts; a model space (P) and an orthogonal space (Q). The basic idea of such a division is to find an effective operator which act only within the limited model space but which generate the same result as do the original operators acting on the entire functional space. Here in the sections which follow, we derive an effective operator for allowed and PNC induced $E1$ transitions using perturbation theory.

2.1. General form of an effective operator for allowed $E1$ transitions

We start the derivation with the total Hamiltonian as

$$H = H_0 + V_{es} \quad (1)$$

where H_0 and V_{es} are the unperturbed one-electron and perturbed two-electron operators. If $|\Psi_0\rangle$ is the atomic state function (ASF), then it satisfies the equation,

$$H_0|\Psi_0\rangle = E_0|\Psi_0\rangle. \quad (2)$$

where E_0 is the energy eigenvalue of the ASF. Here we are interested in allowed $E1$ dipole transitions between the eigen states of the atomic Hamiltonian H as given by

$$E1 = \langle \Psi_\beta | D | \Psi_\alpha \rangle \quad (3)$$

where α and β denotes two different ASFs of different parity and D the dipole operator. Considering Ω as the wave operator which upon acting on an unperturbed part generates the exact state, the observable $E1$ reduces to

$$E1 = \langle \Psi_\beta^{(0)} | \Omega'' D \Omega' | \Psi_\alpha^{(0)} \rangle \quad (4)$$

Here, Ψ_α and Ψ_β denotes the initial and final atomic state functions. Once Ω is known, $E1$ can be computed. Starting from Bloch equation¹ and considering only

terms of different orders in Coulomb interactions, we get $E1$ with D_{eff} operator defined as

$$D_{eff} = \sum_{m=0}^{\infty} [\Omega''^{(m)}]^\dagger D \sum_{n=0}^{\infty} [\Omega'^{(n)}] \quad (5)$$

where $\Omega_{es}^{m,n}$ refers to the wave operator with different orders of the residual Coulomb interaction denoted by m and n corresponding to the initial and final states. We consider D_{eff} to have only connected diagrams. By putting $n = 0$ and $m = 0$, it can be verified that it reduces to unperturbed contribution. Hence, a very general effective operator can be rewritten as

$$D_{eff}^{(n)} = \sum_{m=0}^n [\Omega''^{(m)}]^\dagger D [\Omega'^{(n-m)}]. \quad (6)$$

Hence $E1$ to any order n is given by

$$E1^{(n)} = \langle \Psi_\beta^{(0)} | D_{eff}^{(n)} | \Psi_\alpha^{(0)} \rangle. \quad (7)$$

For $E1^{(1)}$ with one order in Coulomb interaction, $D_{eff}^{(1)}$ reduces to

$$D_{eff}^{(1)} = DR'V_{es}\hat{P} + (R''V_{es}\hat{P})^\dagger D \quad (8)$$

where R' and R'' are the resolvent operators given by

$$\begin{aligned} R' &= \sum_{\gamma \notin M} \frac{|\Phi_\gamma\rangle\langle\Phi_\gamma|}{E_\alpha - E_0^\gamma} \\ R'' &= \sum_{\gamma \notin M} \frac{|\Phi_\gamma\rangle\langle\Phi_\gamma|}{E_\beta - E_0^\gamma}. \end{aligned} \quad (9)$$

Here α, β are in the model (P) and γ in the orthogonal (Q) space with E defining their corresponding eigenvalues and M being the dimension of the model space considered. Considering the ASFs (α, β) to be single determinant with single open valence shell we consider diagrams only of the form given in Fig. 1. The zeroth

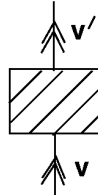


Fig. 1. Form of the diagram for $E1$ with v and v' denoting valence lines.

order $E1$ diagrams are represented in Fig. 2. Here diagrams (2b) and (2c) denote the direct and the exchange parts respectively and diagrams (2d) and (2e) their Hermitian conjugate parts. Higher order $E1$ diagrams can be obtained by taking

4 Geetha Gopakumar et al

different orders of $D_{eff}^{(n)}$ terms and contracting by Wick's theorem to obtain diagrams only of the form given in Fig. 1. In the next section, we follow similar derivation by taking PNC as an additional perturbation along with Coulomb operator.

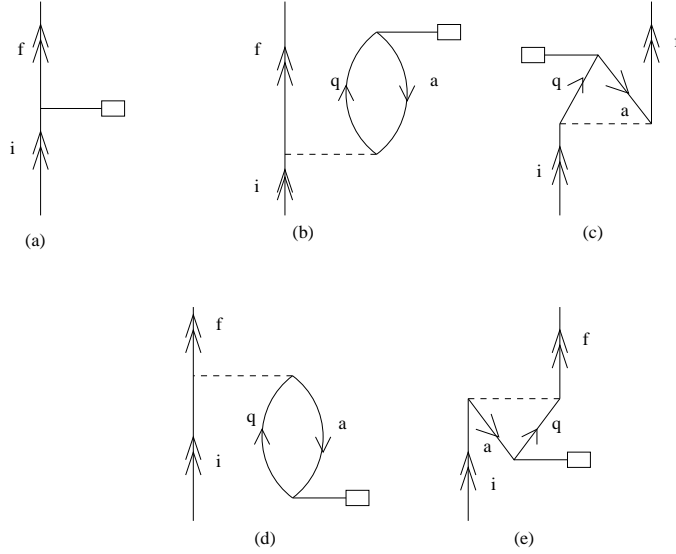


Fig. 2. Diagrams representing $E1^{(1)}$ contributions with diagrams (2b) and (2c) denoting the direct and exchange contributions with diagrams (2d) and (2e) with their Hermitian conjugate part. Here square sign represents Dipole and the dotted lines denotes Coulomb operator. Fig (2a) corresponds to the Dirac-Fock part.

2.2. General form of effective operator for PNC induced allowed $E1$ transitions

We start the derivation with the total Hamiltonian as

$$H = H_0 + V_{es} + H_{PNC} \quad (10)$$

where V_{es} and H_{PNC} are two-electron and one-electron operators and H_{PNC} is expressed as

$$H_{PNC} = \frac{G_F}{2\sqrt{2}} Q_W \sum_e \gamma_5^e \rho(r_e), \quad (11)$$

with

$$Q_W = 2 [ZC_{1p} + NC_{1n}]. \quad (12)$$

Here Z and N are the number of protons and neutrons respectively and C_{1p} and C_{1n} are the vector (nucleon) - axial vector (electron) coupling coefficients whereas

G_F is the Fermi coupling constant and $\rho(r_e)$ is the normalised nucleon number density. The matrix element of H_{PNC} scales as Z^3 . Treating H_{PNC} as a first order perturbation, an ASF can be written as a state of mixed parity.

$$|\tilde{\Psi}\rangle = |\Psi^{(0)}\rangle + |\Psi(\text{corre})\rangle \quad (13)$$

where $|\Psi^{(0)}\rangle$ denotes the unperturbed part which is even/odd under parity and $|\Psi(\text{corre})\rangle$ denotes the correction due to the perturbation which is opposite in parity with respect to the unperturbed part. Due to the mixing of parity in the ASFs, one can expect a non zero electric dipole transition amplitude between states of same parity denoted by $E1PNC$ as given by

$$E1PNC = \langle \tilde{\Psi}_\beta | D | \tilde{\Psi}_\alpha \rangle \quad (14)$$

where α and β denotes two different ASFs. Let us consider that we have only one parity(even+/odd-) in the model space. Considering Ω as the wave operator which upon acting on an unperturbed part generates the exact state, the observable $E1PNC$ reduces to

$$E1PNC = \langle \Psi_\beta^{+(0)} | \Omega^{+''} D \Omega' | \Psi_\alpha^{+(0)} \rangle \quad (15)$$

where the single and double prime on Ω denotes the perturbation on the initial and final states. Once Ω is known, $E1PNC$ can be computed. Starting from Bloch¹ equation, a very general effective operator for various orders of residual Coulomb interaction with one order in H_{PNC} can be derived similar to the previous case. Defining Ω_{es} with various orders of residual Coulomb interaction and Ω_{PNC} with one order in H_{PNC} and different orders of residual Coulomb interaction, we can derive the general effective operator as

$$D_{eff}^{(n)} = \sum_{m=0}^n [\Omega_{es}^{(m)} + \Omega_{PNC}^{(m)}]^\dagger D [\Omega_{es}^{(n-m)} + \Omega_{PNC}^{(n-m)}]. \quad (16)$$

where m and n refers to various orders of perturbation on initial and final states. For $n = 1$ with one order in H_{PNC} and zero orders of residual Coulomb interaction, $D_{eff}^{(1)}$ reduces to

$$D_{eff}^{(1)} = DR' H_{PNC} \hat{P} + (R'' H_{PNC} \hat{P})^\dagger D$$

where R and R' are defined as in the above case. By considering the ASFs to be single determinant with single open valence line and the fact that D and H_{PNC} are single particle operators, we consider diagrams only of the form given by Fig.1. All the possible zeroth and first order diagrams with the corresponding expressions are given in reference⁴. Out of that we are interested only in the RPA kind of diagrams which can be represented as linear equation starting from Hartree Fock (HF) equation and solved to all orders of residual Coulomb interactions.

3. Core Polarisation effects (RPA) in MBPT

Core polarisation effects arise from the residual Coulomb interaction which is treated as a perturbation in MBPT. At each order of perturbation there is a single excitation from the core. The remaining correlation effects involving multiple excitations will not be discussed in this work. In RPA^{5,6,7} theory, the core electrons get perturbed in the presence of an oscillating electric field. By taking these orbital modifications into account in DF potential leads to coupled equations for the electric dipole perturbed functions. In the subsections below, we show the equivalent terms/diagrams for the above effects in MBPT.

3.1. RPA effects in MBPT for allowed E1 transitions

The E1 transition amplitude has been given earlier in Eq.(3). This transition amplitude in the zeroth and first order can be expressed as

$$E1^{(0)} = \langle \Psi_\beta^{(0)} | D | \Psi_\alpha^{(0)} \rangle \quad (17)$$

and

$$E1^{(1)} = \langle \Psi_\beta^{(0)} | D | \Psi_\alpha^{(1)} \rangle + \langle \Psi_\beta^{(1)} | D | \Psi_\alpha^{(0)} \rangle \quad (18)$$

respectively. Using the general diagrammatic rules, all the possible diagrams of the form given in Fig. 1 can be obtained. This is given in Fig. 2. Converting the diagrams to expressions, we get

$$E1_{fi}^{(0)} = \langle f | D | i \rangle \quad (19)$$

and

$$E_{fi}^{(1)} = \sum_{aq} \frac{\langle fq | \tilde{V}_{es} | ia \rangle \langle a | D | q \rangle}{\epsilon_a - \epsilon_q + \epsilon_i - \epsilon_f} + \sum_{aq} \frac{\langle fa | \tilde{V}_{es} | iq \rangle \langle q | D | a \rangle}{\epsilon_a - \epsilon_q - \epsilon_i + \epsilon_f} \quad (20)$$

Here, we define a and q to be core and virtual orbitals with their corresponding single particle orbital energies denoted by ϵ . Tilde on V_{es} refers to the inclusion of exchange terms. From the above expression, it is clear that due to residual Coulomb interaction at first order the core orbital ‘ a ’ is excited to a virtual orbitals defined as ‘ q ’. Hence the above expression denotes the first order RPA contribution in MBPT for allowed E1 transitions. Defining $\omega = \epsilon_f - \epsilon_i$, the higher order RPA diagrams can be obtained by solving the recursive relation as given by

$$E_{fi}^{(n)} = \sum_{aq} \frac{\langle fq | \tilde{V}_{es} | ia \rangle E_{aq}^{(n-1)}}{\epsilon_a - \epsilon_q - \omega} + \sum_{aq} \frac{\langle fa | \tilde{V}_{es} | iq \rangle E_{qa}^{(n-1)}}{\epsilon_a - \epsilon_q + \omega} \quad (21)$$

where n denotes the order of residual Coulomb interaction. Determining the above equation to self consistency first for core to virtual amplitudes and then using it for valence to virtual amplitudes is equivalent to taking all the RPA diagrams of the kind represented in Fig. 3 to all orders.

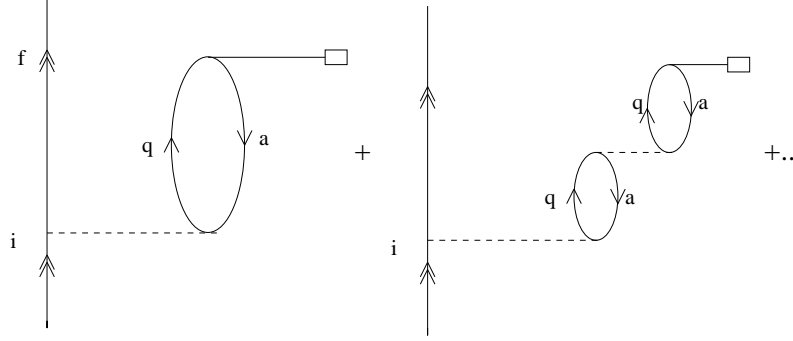


Fig. 3. The kind of RPA diagrams which are solved to all orders by representing the effects as linear equation and solving to self-consistency. Exchange and Hermitian conjugate diagrams are also included.

3.2. RPA effects in MBPT for PNC induced E1 transitions

The influence by an external oscillating electric field on the single particle orbitals of an atom can be obtained by solving DF equation in that field. By taking the matrix elements of the PNC operator between these perturbed states gives rise to the electric dipole transition amplitude which we are interested in. In the lowest order, we get

$$E1PNC^{(1)} = \langle f^D | H_{PNC} | i \rangle + \langle f | H_{PNC} | i^D \rangle \quad (22)$$

where we have defined

$$|(i, f)^D\rangle = \sum_I \frac{|I\rangle \langle I | D | (i, f) \rangle}{(\epsilon_{(i,f)} - \epsilon_I)} \quad (23)$$

Here ϵ_I denotes the intermediate single particle energy. With additional mathematical manipulations (as given in reference⁴) one can derive the all order RPA equation which in turn can also be represented as a linear equation and solved to all orders. The lowest order RPA contribution is shown in Fig. 4. Similarly by taking one order in residual Coulomb interaction, the second order electric dipole transition amplitude takes the form

$$\begin{aligned} E1PNC^{(2)} = & \sum_p \frac{\langle f | H_{PNC} | p \rangle \langle p | D | i \rangle}{(\epsilon_i + \omega - \epsilon_p)} \\ & + \sum_{paq} \frac{\langle f | H_{PNC} | p \rangle \langle pa | \tilde{V}_{es} | iq \rangle \langle q | D | a \rangle}{(\epsilon_i + \omega - \epsilon_p)(\epsilon_a + \omega - \epsilon_q)} \\ & - \sum_{paq} \frac{\langle f | H_{PNC} | p \rangle \langle pq | \tilde{V}_{es} | ia \rangle \langle a | D | q \rangle}{(\epsilon_i + \omega - \epsilon_p)(\epsilon_q + \omega - \epsilon_a)} \end{aligned} \quad (24)$$

with 'p,q' and 'a' refers to virtual and core orbitals. The above equation describes the first order RPA effect as it involves the excitation of the core orbital 'a' to a

8 Geetha Gopakumar et al

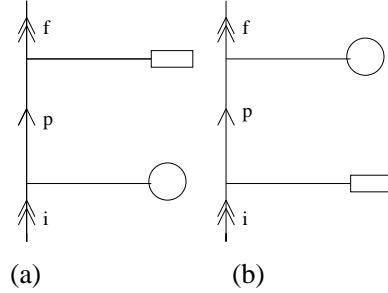


Fig. 4. Diagrams representing $E1PNC^{(1)}$ expression for RPA effects. The square and circle denotes dipole and PNC respectively.

virtual orbital ‘q’ through the residual Coulomb interaction. The difference lies in the presence of the H_{PNC} perturbation acting either on the initial or final states. Comparing diagrammatically, the first and second terms of Eq. (24) is equivalent to

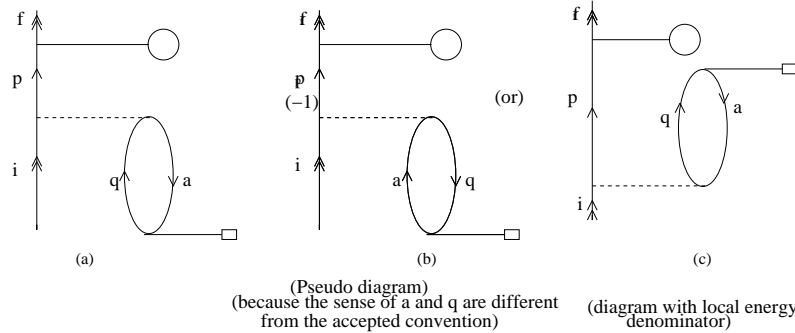


Fig. 5. Diagrams representing $E1PNC^{(2)}$ expression for RPA effects with square and circle sign representing dipole and PNC perturbations. The dotted line denotes Coulomb interaction.

the RPA diagram in Fig. (4a) and (5a) respectively. The third term is represented in two different ways as RPA diagrams in Figs.(5b) and (5c). In the first case, in Fig. (5b), the sense of the core and particle is different from the accepted convention with respect to D vertex and hence it is called a pseudo diagram. Whereas in the second case, by taking the negative sign inside the expression for $E1PNC^{(2)}$, Fig. (5c) can be interpreted by local energy denominator for both D and Coulomb vertex.

Comparing the above terms with all the first order MBPT terms as discussed in ⁴, we can find that the pseudo/local energy denominator diagram can be obtained by adding two MBPT diagrams as shown in Figs. (6b) and (6c) respectively. Similarly, the Hermitian conjugate pseudo diagram can also be obtained by adding the corresponding Hermitian conjugate MBPT diagrams. Fig. (6a) represents the normal RPA diagram as in the Fig. (5a).

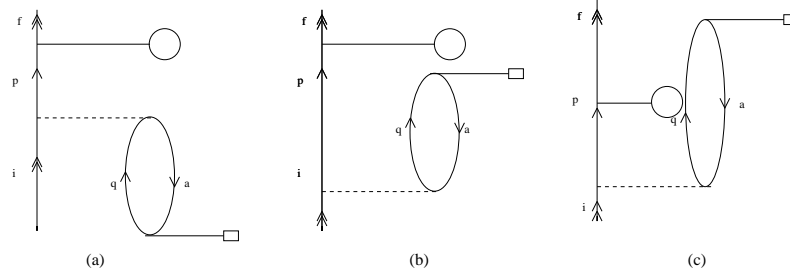


Fig. 6. MBPT diagrams corresponding to RPA. MBPT(1) corresponds to the normal RPA diagram. MBPT(2) and MBPT(3) are added to get the second term of the $E1PNC^{(2)}$ expression for RPA or in other words the pseudo/local energy denominator diagram.

Similar to the allowed $E1$ transition, in the case of PNC, the influence of H_{PNC} as a perturbation can be treated in the framework of RPA. In the next section, we show the basic formulation for CC method and show how RPA terms arises in the above mentioned method.

4. RPA effects in Coupled Cluster (CC) method

We have so far been discussing about perturbation theory in which some of the terms of the perturbation theory were grouped together and evaluated to all orders. This is similar in spirit to the Coupled Cluster method where a particular class of MBPT diagrams is calculated to all orders in the residual Coulomb interaction.

The many-electron wave function in CC method is given by

$$|\Psi_0\rangle = e^{(T)}\{e^S\}|\Phi_0\rangle, \quad (25)$$

where $|\Phi_0\rangle$ is the reference state and T and S are the cluster operators which considers excitations from core and valence to virtual orbitals.

The Hamiltonian in the presence of the PNC weak interaction is given by

$$H = H_a + H_{PNC} \quad (26)$$

where H_a and H_{PNC} denotes the atomic Hamiltonian and the PNC perturbation with G_F showing the strength of the perturbation. Hence

$$\begin{aligned} T &= T^{(0)} + G_F T^{(1)}, \\ S &= S^{(0)} + G_F S^{(1)}. \end{aligned}$$

Here we denote the T and S with a superscript ‘0,1’ as unperturbed and as PNC perturbed cluster amplitudes. Once the cluster amplitudes are computed, $E1PNC$ can be obtained by taking one order in H_{PNC} perturbation in initial/final states either through T or S cluster amplitudes⁹ connected by the D operator. Whereas for the allowed $E1$ calculations, the unperturbed cluster amplitudes in the initial/final states are connected by the D operator. In the sections below, the RPA diagrams

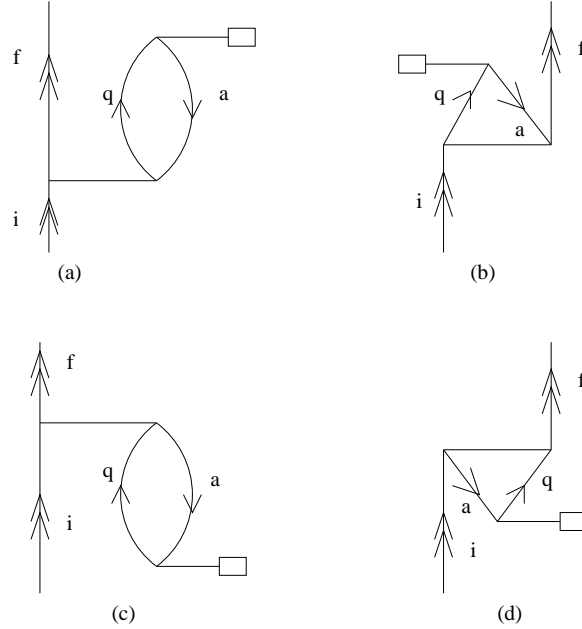


Fig. 7. Coupled cluster counter part of fig 2. Here the dotted line is replaced by a solid line representing an all-order Coulomb interaction vertex.

are compared both diagrammatically and numerically with CC for allowed $E1$ transitions.

4.1. Diagrammatic comparison of RPA diagrams corresponding to CC diagrams for allowed and PNC induced $E1$ transitions

We now consider CC diagrams corresponding to the RPA effects. In CC theory for allowed and PNC perturbed dipole transitions, we consider D as an operator. The Coulomb operator acts as a perturbation for the allowed transitions, whereas for the PNC induced $E1$ transitions, we have PNC perturbation in addition to it. Therefore we need to first find out from which side of the dipole operator the perturbations act.

The diagrams for the allowed $E1$ transition amplitude in the framework of CC theory has been discussed in one of our earlier papers⁸. The RPA diagrams given in Figs. (2b-2e) correspond to the DS_2 and $S_2^\dagger D$ diagrams of CCT (See Fig 7). In the case of PNC induced $E1$ transitions, the MBPT diagram (4a) and (4b) in Fig. 4 corresponding to zeroth order RPA effects can be got from $DS_1^{(1,0)}$ where the superscripts denotes the order in PNC and the residual Coulomb interaction in the order of preference. By looking at the regular RPA diagram in Fig. (5a) contributing to first order in Coulomb and PNC, we find that it is equivalent to $DS_2^{(1,1)}$ diagram and its Hermitian conjugate in CC theory. Whereas the pseudo/local energy

denominator diagram, which is shown as equivalent to addition of MBPT diagrams in Fig. (6b) and (6c) can be got from the term $S_1^{\dagger(1,0)} DS_2^{(1,0)}$ and its Hermitian conjugate respectively.

By comparing the terms in CC method for allowed and PNC induced E1 transitions, we find that the additional diagrams arises solely due to the presence of PNC operator acting either on the incoming or the final vertex. We find that PNC acting on the same vertex as Coulomb operator, leads to the regular diagram and PNC and the residual Coulomb interaction on the initial and final vertices leads to the additional pseudo/local energy diagram.

5. Numerical comparison of RPA diagrams corresponding to CC diagrams for allowed E1 transitions

In order to demonstrate that the RPA effects are contained in CCT we have compared the all order RPA results with the sum of DS_2 and $S_2^\dagger D$ contributions in our CC calculations for the allowed $3s^2S_{1/2} \rightarrow 3p^2P_{1/2}$ and $3s^2S_{1/2} \rightarrow 3p^2P_{3/2}$ transitions in Na^+ . We first generate the single particle DF orbitals with $Na^+(2p^6)$ as the starting potential. The GTOs were generated using the Finite Basis Set Expansion (FBSE) method¹⁰ with a primitive basis set consisting of 35s-32p-25d-25f. With appropriate energy cutoffs in the discrete core and continuum virtual orbital spectrum, the calculation was done with 11s-10p-9d-8f basis.

$3s \rightarrow 3p_{1/2}$		$3s \rightarrow 3p_{3/2}$	
RPA	RPA-CC	RPA	RPA-CC
0.044	0.044	-0.061	-0.062

Table 1. Comparative results of E1 reduced matrix elements (in *a.u.*) arising from RPA and RPA-CC ($DS_2 + S_2^\dagger D$) for $3s \rightarrow 3p_{1/2}$ and $3s \rightarrow 3p_{3/2}$ transitions in Na^+ .

As stated earlier DS_2 and $S_2^\dagger D$ terms in CCT (Fig. 7) correspond to the RPA diagrams given in Figs. (2b-2e). In table 1 we give the numerical values of those two contributions for $3s \rightarrow 3p_{1/2}$ and $3s \rightarrow 3p_{3/2}$ transitions in Na^+ . As expected the agreement between the two results is very good.

6. Conclusion

Using analytical and diagrammatic techniques we have identified the RPA effects in allowed and parity non-conserving electric dipole transition amplitudes. We have demonstrated that these effects arise in MBPT and CCT. Indeed the all order RPA contribution is subsumed in CCT.

7. Acknowledgements

The present research was partly done at Indian Institute of Astrophysics, when the author (GG) was completing her PhD work. This work was completed later at University of Tokyo with the support from National Institute of Advanced Industrial Science and Technology (AIST) and later by National Research Grid Initiative (NAREGI) of Ministry of Education, Culture, Sports, Science and Technology (MEXT), Japan. One of the authors (CS) acknowledges the BRNS for project no. 2002/37/12/BRNS.

1. I.Lindgren and J. Morrison, *Atomic Many-Body Theory*, Second Edition, Springer Verlag, p.356(1986)
2. D.J.Rowe, *Rev.Mod.Phys.*, **40**, 153(1968) and references therein, A.Dalgarno and G.A.Victor *Proc.R.Soc.A*, **291**,291(1966)
3. E.D.Commins, P.H.Bucksbaum, *Weak Interactions in Quarks and Leptons*, Cambridge University Press, London (1973).
4. Geetha Gopakumar, Bhanu Pratap Das, Rajat Chaudhuri, D. Mukherjee and K. Hirao (submitted to Physical Review A)
5. A. M. Martensson-Pendrill, *J.Physique*, **46**, 1949(1985)
6. P. G. H. Sandars, *J. Phys. B*, **10**, 2983 (1977).
7. V. A. Dzuba, V. V. Flambaum, Silverstov and O. P. Sushkov, *J. Phys. B*, **18**, 597 (1985).
8. G.Gopakumar, H.Merlitz, R.K.Chaudhuri, B.P.Das, U.S.Mahapatra and D.Mukherjee, *Phys. Rev. A*, **66**,032505 (2002).
9. Bijaya Kumar Sahoo, PhD thesis submitted to Mangalore University (2005).
10. Rajat K. Chaudhuri, P.K.Panda and B.P.Das, *Phys.Rev.A*, **59**, 1187 (1999)